

Probing the centre of the large circumstellar disc in M 17^{*}

M. Nielbock,^{1†} R. Chini,² V. H. Hoffmeister,² D. E. A. Nürnberger,³
C. M. Scheyda² and J. Steinacker^{1,4}

¹Max-Planck-Institut für Astronomie, Königstuhl 17, D-69117 Heidelberg, Germany

²Astronomisches Institut der Ruhr-Universität Bochum, Universitätsstraße 150/NA 7, D-44780 Bochum, Germany

³European Southern Observatory, Alonso de Cordova 3107, Casilla 19001, Santiago 19, Chile

⁴Astronomisches Rechen-Institut, Zentrum für Astronomie Heidelberg, Mönchhofstr. 12-14, D-69120 Heidelberg, Germany

Received / Accepted

ABSTRACT

We investigated the nature of the hitherto unresolved elliptical infrared emission in the centre of the $\sim 20\,000$ AU disc silhouette in M 17. We combined high-resolution $JHKsL'M'$ band imaging carried out with NAOS/CONICA at the VLT with [Fe II] narrow band imaging using SOFI at the NTT. The analysis is supported by Spitzer/GLIMPSE archival data and by already published SINFONI/VLT Integral Field Spectroscopy data. For the first time, we resolve the elongated central infrared emission into a point-source and a jet-like feature that extends to the northeast in the opposite direction of the recently discovered collimated H₂ jet. They are both orientated almost perpendicular to the disc plane. In addition, our images reveal a curved southwestern emission nebula whose morphology resembles that of the previously detected northeastern one. Both nebulae are located at a distance of 1500 AU from the disc centre. We describe the infrared point-source in terms of a protostar that is embedded in circumstellar material producing a visual extinction of $60 \leq A_V \leq 82$. The observed Ks band magnitude is equivalent to a stellar mass range of $2.8 M_\odot \leq M_* \leq 8 M_\odot$ adopting conversions for a main-sequence star. Altogether, we suggest that the large M 17 accretion disc is forming an intermediate to high-mass protostar. Part of the accreted material is expelled through a symmetric bipolar jet/outflow.

Key words: stars: formation, circumstellar matter, pre-main sequence – infrared: stars – ISM: individual: M 17

1 INTRODUCTION

The processes forming high-mass stars are still not well understood. Although recent theoretical models require the presence of and the accretion from a circumstellar disc (Bonnell et al. 2001; Yorke & Sonnhalter 2002; Krumholz, Klein & McKee 2007), the direct observation of such a configuration is still missing.

During a systematic infrared study of the young star cluster NGC 6618 inside the H II region M 17 (Omega Nebula), Chini et al. (2004) discovered an opaque silhouette, shaped like a flared disc at JHK with a diameter of $\sim 20\,000$ AU against the bright background of the H II region. It is associated with an optically visible hourglass-shaped nebula perpendicular to the silhouette plane. The

optical spectrum of the nebula exhibits emission lines with blue-shifted absorption features indicating disc accretion.

Steinacker et al. (2006) successfully modelled the optical depth and the photon scattering of the silhouette at $2.2\ \mu\text{m}$ and obtained a large circumstellar disc seen at an inclination angle of 12° (almost edge-on). They found disc masses between 0.02 and $5 M_\odot$ depending on the assumed dust model and the distance. The mass range is in good agreement with the distance-scaled values by Sako et al. (2005) derived from their NIR (near infrared) extinction map. The distance has recently been determined to 2.1 ± 0.2 kpc on the basis of about 50 spectroscopically classified early-type stars (Hoffmeister et al. 2008) ruling out earlier estimates below 2 kpc that treated several unresolved high-mass binaries as single stars. The new spectro-photometric distance agrees well with previous studies based on multi-colour photometry (2.2 ± 0.2 kpc; Chini, Elsässer & Neckel 1980) and radio data ($2.4 \pm_{0.5}^{0.4}$ kpc; Russeil 2003).

Independent of its mass, the M 17 silhouette is the

^{*} Based on observations collected at the European Southern Observatory, Chile., project nos. 73.C-0170, 73.C-0183 and 75.C-0852.

[†] E-mail: nielbock@mpia.de

largest disc found to date that is exhibiting accretion activity. In fact, Nürnbergger et al. (2007) discovered a H₂ jet emerging from the disc centre, also suggesting ongoing accretion.

At the disc centre, Chini et al. (2004) found an elliptical *K* band emission of $240 \times 450 \text{ AU}^2$. Likewise, Sako et al. (2005) describe the central object as an elongated compact infrared source. A faint emission of unknown nature is also visible in their [Ne II] narrow band MIR (mid infrared) image at $12.8 \mu\text{m}$.

Assuming that the central *K* band flux found by Chini et al. (2004) originates from a single star at a distance of 2.1 kpc, the stellar mass may range between a few and $45 M_{\odot}$, depending on the extinction model (Steinacker et al. 2006). Sako et al. (2005) explained their results in terms of an intermediate-mass object with a stellar mass of 2.5 to $8 M_{\odot}$. Their analysis was part of a larger survey of candidate silhouette objects in M17 (Ito et al. 2008).

So far, both the mass and the temperature of the forming star within this spectacular disc remain under discussion. In this work, we present new data that provide further insight into the nature of the central protostellar object and constrain the possible mass range. We also discuss the detection of a possible counter-jet headed in the opposite direction of the H₂ jet and a curved southwestern emission nebula that is geometrically symmetric to the northeastern one.

2 OBSERVATIONS AND REDUCTION

The narrow band imaging was done with SOFI (Finger et al. 1998) at the ESO NTT on La Silla, Chile, in April 2004. The [Fe II] line at $\lambda = 1.64 \mu\text{m}$ was probed with a narrow band filter centred on $\lambda = 1.644 \pm 0.025 \mu\text{m}$. In order to subtract the continuum from the spectral line data, we obtained images in an adjacent narrow band filter centred on $\lambda = 1.71 \mu\text{m}$. The seeing limited spatial resolution is $0''.9$ (FWHM), the pixel size is $0''.288$.

The adaptive optics *JHKsL'M'* imaging was carried out in July and August 2005 with NAOS/CONICA (Rousset et al. 2003; Hartung et al. 2003) at the ESO VLT. We used the CONICA S13 lens for the *JHKs* measurements providing a pixel resolution of $0''.013$ and a field size of $14'' \times 14''$. The *L'M'* imaging was done with the L27 lens resulting in a pixel size of $0''.027$. While for the *L'* band the corresponding FOV was $28'' \times 28''$, *M'* band measurements only use the central 512×512 pixels equivalent to a field size of $14'' \times 14''$. The effective spatial resolution is $0''.1$ (FWHM). The photometric errors vary between 0.1 mag and 0.4 mag.

The Spitzer post-BCD data were taken from the GLIMPSE survey archive (Benjamin et al. 2003) based on an imaging campaign of the galactic plane using the IRAC camera (Fazio et al. 2004) on board the Spitzer infrared satellite (Werner et al. 2004).

All data were reduced and analysed with IRAF and MOPSI; the NACO *H* and *Ks* band images are shown in Fig. 1. Among the NIR AO data, only the *Ks* band image shows a point-source; at *J* and *H* the emission is diffuse and extended. It was not detected at all in the *L'M'* bands. Therefore, establishing a meaningful SED (spectral energy distribution) for the embedded source is difficult. We

Table 1. NACO multi-colour photometry of the central source.

λ_c [μm]	Point-source		NE tail	
	m [mag]	F [μJy]	m [mag]	F [μJy]
1.27	> 23.71	< 0.5	> 23.71	< 0.5
1.66	> 20.74	< 7.1	> 20.74	< 7.1
2.18	19.28 ± 0.07	12.9 ± 0.9	20.10 ± 0.12	6.1 ± 0.7
3.80	> 13.67	< 960	> 13.67	< 960
4.78	> 12.61	< 1460	> 12.61	< 1460

were able to produce adequate PSF models in the NACO *HKsL'M'* bands by selecting 6 to 10 sufficiently bright stars also detected on the same frame for the subsequent PSF photometry. Within the errors, the *Ks* PSF fit to the central point-source appeared circular. The surrounding fuzzy and somewhat scattered emission can be entirely attributed to the central ridge introducing a background pattern similar to what is visible in the *H* band. Due to the absence of sufficiently bright PSF model stars in the NACO *J* band, we had to perform aperture photometry. An aperture correction was applied to all the measurements. The results of the photometry are listed in Table 1.

Astrometric calibration of all but the NACO data is based on the 2MASS database. Since there are no 2MASS sources on the NACO frames, we used stars detected with ISAAC (Chini et al. 2004) in the vicinity of the disc for astrometry. We estimate the accuracy to be better than $0''.1$.

3 RESULTS AND DISCUSSION

3.1 The central point-source

The *Ks* band image in Fig. 1 for the first time resolves the elliptical infrared emission at the disc centre into a point-source with a FWHM of $0''.1$ (210 AU) and a tail that extends to the northeast. We regard the point-source as a single object, although close high-mass binaries can be separated by $\leq 0.25 \text{ AU}$ (Krumholz & Thompson 2007). The peak of the tail emission is separated by $0''.08$ (170 AU) from the point-source, defining a line that we interpret as the outflow axis (see Sect. 3.2). It appears tilted by $\sim 15^\circ$ from the disc symmetry axis. In the *H* band, we only detect diffuse emission without any indication for a point-source.

The symmetry of the source-jet-disc configuration is striking. In particular the link between the source and the jet seems obvious. The point-source bisects the line between the peak emission of the northeastern nebula coinciding with a weak H₂ feature and the first strong maximum of the jet to the southwest (Fig. 1, right panel). If chosen as the symmetry centre of the bipolar nebula, both wings match perfectly when rotated by 180° (Fig. 1, left panel).

Assuming the point-source emission stems from a reddened stellar photosphere at a distance of 2.1 kpc, we can combine our photometry with the extinction estimate of Steinacker et al. (2006). They pursued the so far most sophisticated approach to model the spatial distribution of the optical depth of the disc at $2.2 \mu\text{m}$ up to an outer radius of 10 000 AU including photon scattering effects. Their result of $\tau_{2.2 \mu\text{m}} = 2.6$ ($A_V = 27$) toward the disc centre is a lower limit, because (a) the unresolved inner disc at

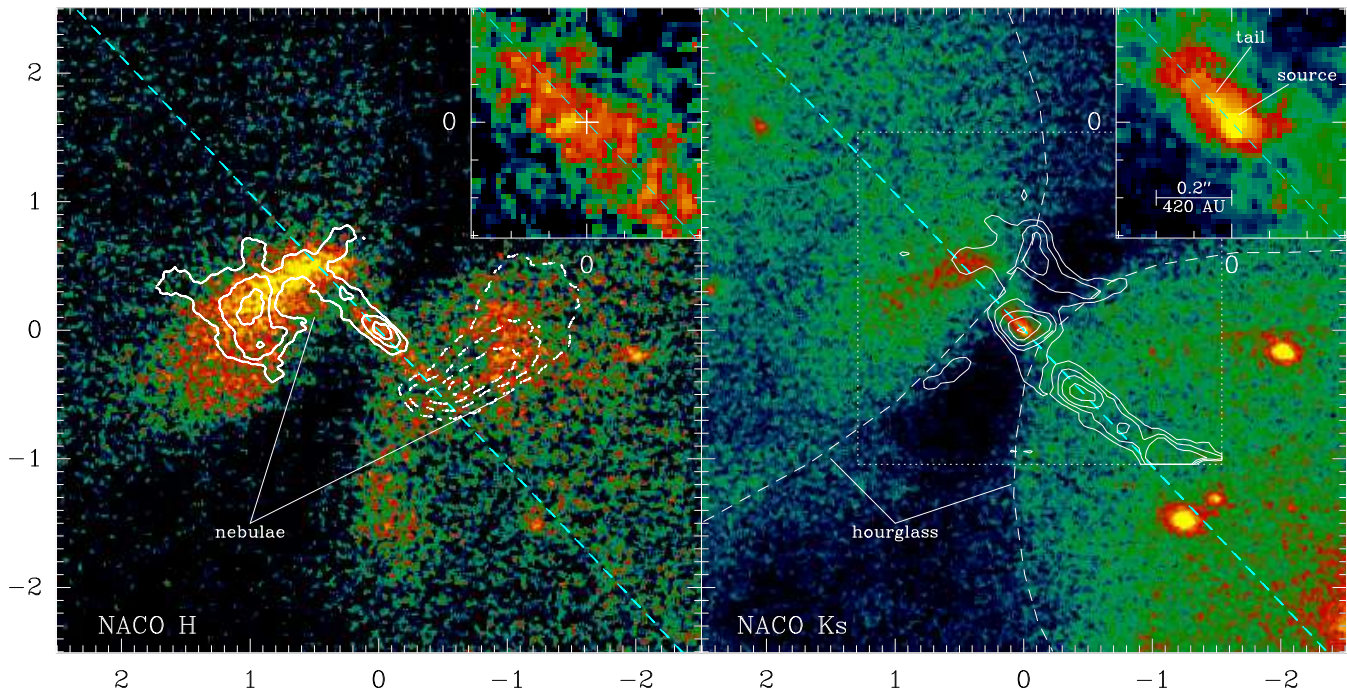


Figure 1. Infrared images of the inner region ($5'' \times 5''$) of the M17 disc silhouette centred on the newly detected point-source at R.A. = $18^{\text{h}}20^{\text{m}}26^{\text{s}}.191$ and Dec. = $-16^{\circ}12'10''.46$ (J2000). The inserts enlarge the central $0''.6 \times 0''.6$. Left: H image showing the symmetric bipolar nebula. The central point-source is not detected. To visualise the symmetry of the two nebulae, we have superimposed their contours after rotating them by 180° around the central point-source which we define as the symmetry centre; solid contours refer to the southwestern lobe, dashed contours represent the northeastern one. The hourglass structure above and below the disc hosts the bipolar nebula, of which the southwestern lobe is not detected. The contours denote the continuum-free H_2 $1-0\text{S}(1)$ line emission at $\lambda = 2.12 \mu\text{m}$ as published by Nürnberg et al. (2007); the dotted box delineates the extent of the H_2 image. The dashed blue lines mark the suggested jet axis as determined by the orientation of the detected tail with respect to the point-source.

radii of ≤ 1000 AU were excluded from the model, and (b) the model accounts for the optical depth of the disc alone without the influence of interstellar and intra-cluster foreground extinction. The latter contributions are estimated by analysing the NIR colours of stars in the vicinity of the disc derived from the previously published ISAAC JHK data (Chini et al. 2004). Typical extinction values off the disc plane are about $A_V = 35 \pm 5$. As a result, the sum of the foreground and disc extinction toward the disc centre amounts to $A_V = 62 \pm 5$. Ito et al. (2008) find an absolute upper limit of $A_V = 30$, but this is probably biased by their detection limit. It contradicts previous estimates giving extinction values of $A_V > 40$ for individual stars in this area (Chini & Wargau 1998; Jiang et al. 2002; Hoffmeister et al. 2006).

We also estimated the extinction towards the disc centre independently by creating an extinction map employing the method described by Siebenmorgen & Krügel (2000). It is based on a differential photometry of the attenuating material (the disc) and a uniform background radiation (the H II region). Considering a uniform foreground extinction across the extent of the disc, the measured optical depth is purely due to the material inside the disc, because other contributions along the line of sight like interstellar and intra-cluster extinction or emission cancel out. Using Spitzer/GLIMPSE archival data at 3.6 and $4.5 \mu\text{m}$, we determined the spatial distribution of the optical depth by analysing the attenuation of the background emission originating from the ionised

gas. This approach is comparable to the NIR extinction maps of Sako et al. (2005) and Ito et al. (2008), but it has the advantage of being less susceptible to scattering effects because of the larger wavelengths covered by the Spitzer data. The optical depth estimates were converted to visual extinction values (Flaherty et al. 2007; Román-Zúñiga et al. 2007; Nielbock, Chini & Müller 2003). In the resulting maps (Fig. 2), the extinction maximum is offset by $\sim 3''$ (6300 AU) southeast from the central point-source. Along the line of sight toward the disc centre, we obtain a total extinction solely caused by the disc material of $A_V = 60 \pm 10$, half of which is expected to be the disc extinction toward the centre. The true peak extinction is probably even higher because of the spatial averaging resulting from the limited resolution of the Spitzer data. This leads to a blending of extinction and emission features resulting in a lower limit estimate of the extinction. Ito et al. (2008) find similar displacements between the extinction maximum of candidate silhouette objects and the suggested embedded YSO, which they attribute either to a migration of the YSO or its off-centred formation. However, it is still possible that those identified silhouette structures are not necessarily related to the nearby YSOs. After adding the foreground extinction, our results from the Spitzer extinction maps are consistent with the estimate based on the NIR modelling.

Using the estimate of $A_V \sim 60$ mag as a lower limit to the extinction, the apparent K_s magnitude of the point-source is equivalent to an absolute magnitude of a star hav-

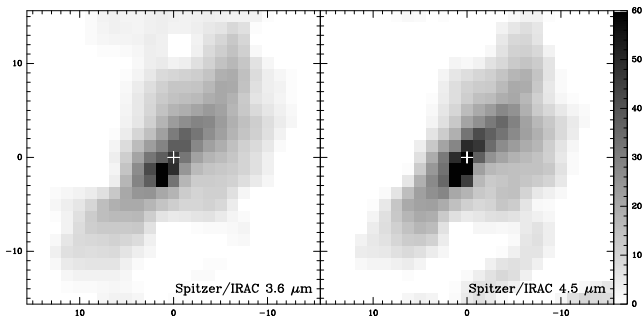


Figure 2. Visual extinction maps of the central $30'' \times 30''$ of the disc determined by applying the method of Siebenmorgen & Krügel (2000) to Spitzer/IRAC data. The position of the central point-source is marked with a white cross. The scale is given in A_V . The extinction maximum is located $\sim 3''$ southeast of the disc centre.

ing a spectral type of at least B8. In the case of a main-sequence star, this would correspond to a stellar mass of $\sim 2.8 M_\odot$ (Blum, Conti & Damiani 2000). Although the reconstructed SINFONI H_2 line image possesses a peak at the disc centre, the contribution of the H_2 emission to the continuum flux is negligible. The continuum flux measured in the NACO K_s filter ($\Delta\lambda = 0.35 \mu\text{m}$) amounts to $2.9 \times 10^{-18} \text{ W m}^{-2}$; the $H_2 1-0\text{S}(1)$ and $H_2 2-1\text{S}(1)$ lines that have been measured with SINFONI contain a continuum corrected line flux of $2-8 \times 10^{-20} \text{ W m}^{-2}$. Thus, they contribute only 1–3% to the continuum flux in the K_s filter. However, we cannot rule out any additional contamination by excess emission of spatially unresolved circumstellar material or accretion signatures close to the protostar.

Sako et al. (2005) present an image of this object obtained in the MIR using a narrow-band filter centred on the $[\text{Ne II}]$ line at $12.8 \mu\text{m}$. Although a faint elongated emission is detected at the disc centre, it does not contribute much to resolving the open question of the nature of the central star. Since emission from this line is commonly observed for circumstellar discs (e. g. Pascucci et al. 2007), it is not clear, how much of the detection is caused by continuum emission.

A strict upper mass limit is difficult to determine from the available data. Sako et al. (2005) argued that the missing radio continuum in the interferometric radio map of Felli, Massi & Churchwell (1984) establishes an upper mass limit of $8 M_\odot$. However, this statement might not be valid, because the source is located in projection onto an ionisation front exhibiting large scale free-free emission that could cause confusion with any weak compact H II source like an early-type star in the lower mass range. Furthermore, a very young and just developing ionised gas sphere (e. g. a hypercompact H II region) would be too small and too weak to be detected by its free-free emission (Kurtz 2005).

In order to address this question, we analysed the NIR colours derived from the values and upper limits given in Tab. 1. Assuming the $K_s - M$ colour is entirely due to a reddened photosphere, the measured upper limit of $K_s - M \leq 6.7$ can be used to set an upper limit on the mass of the protostar. Fig. 3 displays the parameter space of $K_s - M$ colours for given combinations of the visual extinction and the effective temperature of a main-sequence star. The colours were derived from Ducati et al. (2001), and the temperatures are assigned to spectral types and stellar

masses according to Blum et al. (2000). The loci of a reddened main-sequence star with an apparent magnitude of $K_s = 19.28$ is indicated by crosses, interpolated by a solid line. This diagram yields the following two results: First, for the previously determined lower extinction limit of $A_V = 60$ the $K_s - M$ colour attained by extinction alone amounts to 4.9. Hence, any additional NIR colour excess must be less than $K_s - M = 1.8$. Second, the measured $K_s - M$ colour determines the upper extinction limit to $A_V \leq 81.7$. This constrains also the effective temperature to $T_{\text{eff}} \leq 22500 \text{ K}$ which is equivalent to a spectral type just above B1, being in the mass range of about $8 M_\odot$ for a main-sequence star (Blum et al. 2000). In this way, we corroborate the upper mass limit given by Sako et al. (2005). At this point, we want to emphasise that not only the colours but also the photometry and upper limits in Tab. 1 are consistent with these estimates.

3.2 The jet emission

The collimated H_2 jet detected by Nürnberger et al. (2007) originates at the disc centre and extends as far as $3''.6$ to the southwest. The SINFONI data suggest a blue-shifted motion. Correcting for the disc inclination of 12° (Steinacker et al. 2006), a protostellar jet with a typical velocity of 100 km s^{-1} (Reipurth & Bally 2001) would reach the current terminus within 365 years. The expected northeastern counter-jet was not detected by Nürnberger et al. (2007).

The NACO K_s image (Fig. 1, right panel) gives a first hint for the existence of such a feature, because the position angle between the point source and the jet-like feature extending to the northeast agrees with the direction of the H_2 jet. This alignment indicates that we either see the origin of the counter-jet or at least circumstellar matter entrained and heated by its interaction. The northeastern extension of the central H_2 detection by SINFONI that coincides with the jet-like feature may be an indication for residual jet emission. Therefore, we suggest that the counter-jet might exist, but it is strongly extinguished by the circumstellar material. This agrees with the picture suggested by Steinacker et al. (2006) that the near side of the disc is inclined to the northeast and partly covers the latitudes above the disc plane. On the other hand, this jet may fail to produce detectable shocks due to a lack of dense material that has been cleared by the wind and radiation of the cluster OB stars that are mostly located on the northeastern side of the disc.

3.3 The bipolar nebula

The accretion disk is associated with a bipolar hourglass shaped structure (Chini et al. 2004). The northeastern cavity hosts an emission nebula that resembles the working surface of protostellar jets as seen in other outflows like HH 47 (Heathcote et al. 1996; Hartigan et al. 2005). Our new NACO H band image shows a similar, but fainter feature inside the southwestern cavity. In the left panel of Fig. 1, we have superimposed the contours of the northeastern emission onto the southwestern nebula and vice versa after rotating them by 180° . Besides a similar morphology, there is a symmetry of the peak emission with respect to

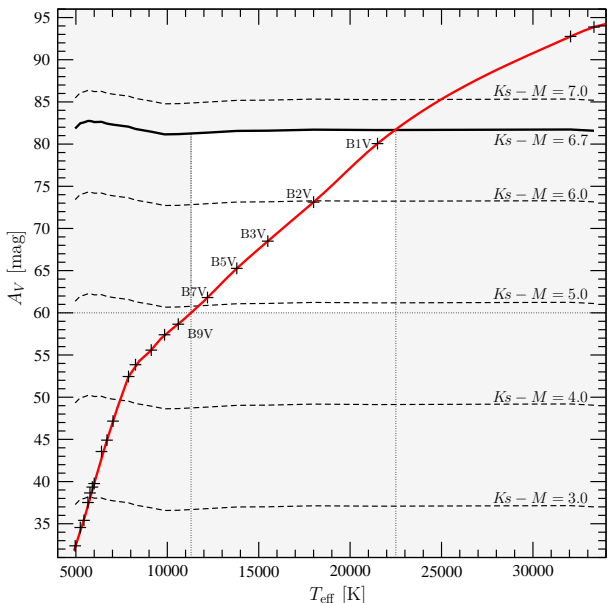


Figure 3. Analysis of infrared colours $Ks - M$ for combinations of effective temperatures of stellar photospheres and visual extinctions. The colours are taken from Ducati et al. (2001). The measured upper limit of $Ks - M \leq 6.7$ is plotted as a solid line resulting in an upper extinction limit of $A_V \leq 81.7$. The lower extinction limit of $A_V \geq 60$ is denoted by the white box. The crosses – interpolated by a solid line – demonstrate the valid range for a reddened main-sequence star of $Ks = 19.28$ at a distance of 2.1 kpc, neglecting excess emission. The temperatures and spectral types are taken from Blum et al. (2000). The resulting valid range determined by $T_{\text{eff}} = 11300 \dots 22500$ K is highlighted by the white box.

the central point-source. Both nebulae have a projected distance of 1500 AU from the central object and their origins are located along an axis that matches the position angle of the star/jet system.

Using its full size at half maximum in the H band, the northeastern nebula covers an opening angle of $\sim 70^\circ$ with respect to the central point-source; it has a projected length of 2500 AU ($1''.2$) and a projected breadth of 840 AU ($0''.4$). In the same area, the NACO data attain $J = 17.59$ mag/ \square'' , $H = 16.68$ mag/ \square'' and $Ks = 16.80$ mag/ \square'' with the brightness peaking along the assumed jet direction. We find an H band excess of > 1.2 mag/ \square'' to what would be expected for the thermal emission of a black body derived from the JHK data. This can be explained either by a combination of scattering and extinction or by line emission.

Radiation from singly ionised iron – together with H_2 – is the main coolant of shocked gas in the NIR (Caratti o Garatti et al. 2006). $[\text{Fe II}]$ lines are commonly observed in J shocks, where the H_2 is completely dissociated (Hollenbach & McKee 1989; Kumar et al. 2003). Therefore, it is a good candidate for contaminating the H band continuum flux. However, apart from a spurious detection of $[\text{Fe II}]$ emission ahead of the northeastern nebula, in our NTT/SOFI narrow band data (not shown) it is strongly concentrated towards the disc centre. This seems to be a typical phenomenon for many protostellar jets (Itoh 2001; Davis et al. 2006). Therefore, the origin of the strong H band emission is probably not caused by $[\text{Fe II}]$.

Another more likely explanation is that the nebulae are scattered light reddened by extinction from the disc material. The spectroscopic accretion signatures (Chini et al. 2004) imply that most of the scattered photons originate from the disc centre. Stark et al. (2006) present Monte Carlo radiative transfer models of circumstellar discs around young stellar objects. They show that NIR colours of the disc centres affected by light scattering and extinction strongly depend on the infall rate, the inclination angle, and the cavity opening angle of the disc. Their models cover infall rates up to $10^{-5} M_\odot \text{ yr}^{-1}$ producing exceptionally blue colours of $H - K = 0.6$ for nearly edge-on discs. Assuming that the accretion rate of the large M17 disc of about $10^{-4} M_\odot \text{ yr}^{-1}$ (Nürnberger et al. 2007) is of the same order as the envelope infall rate, we would expect even bluer colours which is at least qualitatively consistent with our result of $H - Ks = 0.12$.

3.4 H_2 emission at the disc surface

In the right panel of Fig. 1, we have superimposed contours of the SINFONI data of Nürnberger et al. (2007) to compare the highly resolved $H_2 1 - 0S(1)$ emission with the Ks continuum. Apart from the prominent emission from the disc centre and the southwestern jet, there is also molecular hydrogen emission at the position of the northwestern disc lane and – although much weaker – at the northeastern nebula. As the H_2 emission in the disc seems to peak at its surface, an external excitation process like UV pumping might be in action. Indeed, PDRs (photo-dissociation regions) are known to possess a fair amount of molecular hydrogen just below its surface that can be excited by FUV (far ultraviolet, $6 \text{ eV} < h\nu < 13.6 \text{ eV}$) radiation (Tielens & Hollenbach 1985). The existence of such a PDR is also supported by the detection of emission in the Spitzer $8.0 \mu\text{m}$ band that includes PAH bands (polycyclic aromatic hydrocarbon molecules).

Two possible sources for the exciting UV photons have to be considered: (a) the surrounding cluster stars, and (b) the embedded star in the disc centre itself. If excited by the surrounding cluster stars, one would expect the entire disc surface to be a PDR that would be detected by H_2 line emission. However, because the size of the PDR is not only a function of the temperature but also of the density distribution inside the disc, an isotropic UV radiation field does not necessarily result in a uniform PDR. The major emission occurs at the northeastern side of the disc facing the hottest cluster stars. If the PDR is due to the embedded central object, a detailed analysis of the excitation process in the disc could help to further constrain the nature of the forming star.

4 CONCLUSIONS

With the new observations, we have further clarified the nature of the emission in the centre of the large M17 disc and its associated nebula in the following aspects:

- (i) The faint central elliptical emission is resolved for the first time into a point-source and a tail that extends to the northeast. This morphology suggests a single protostar accompanied by a jet.

(ii) The jet-like feature is headed in the opposite direction of a collimated H₂ jet.

(iii) A southwestern emission nebula is turning the outflow pattern from the disc centre into a fairly symmetric morphology. The intensity ratio of the bipolar emission, however, is highly asymmetric, probably due to the inclination of the dusty disc.

(iv) The bipolar nebula might be scattered light which is reddened by extinction caused by the disc material.

(v) Various estimates of the extinction towards the embedded protostar yields a range of $60 \leq A_V \leq 82$.

(vi) The observed 2.2 μm flux is equivalent to a protostar with a mass range of $2.8 M_\odot \leq M_\star \leq 8 M_\odot$.

The new data strengthen the evidence for an intermediate to high-mass protostellar object being formed by accretion.

ACKNOWLEDGEMENTS

We thank the VLT team for performing the *JHKsL'M'* observations in service mode. This work was partly funded by the Nordrhein–Westfälische Akademie der Wissenschaften. M. Nielbock acknowledges the support by the Deutsche Forschungsgemeinschaft, DFG project SFB 591 and the Ministerium für Innovation, Wissenschaft, Forschung und Technik (MIWFT) des Landes Nordrhein–Westfalen. We thank M. Haas for helpful discussions. The constructive response of the anonymous referee is highly appreciated.

This publication makes in part use of data products from the Two Micron All Sky Survey, which is a joint project of the University of Massachusetts and the Infrared Processing and Analysis Center/California Institute of Technology, funded by the NASA and the National Science Foundation.

This work is based in part on observations made with the Spitzer Space Telescope, which is operated by the Jet Propulsion Laboratory, California Institute of Technology under a contract with NASA.

REFERENCES

- Benjamin R. A. et al., 2003, *PASP*, 115, 953
 Blum R. D., Conti P. S., Damineli A., 2000, *AJ*, 119, 1860
 Bonnell I. A., Bate M. R., Clarke C. J., Pringle J. E., 2001, *MNRAS*, 323, 785
 Caratti o Garatti A., Giannini T., Nisini B., Lorenzetti D., 2006, *A&A*, 449, 1077
 Chini R., Elsässer H., Neckel T., 1980, *A&A*, 91, 186
 Chini R., Hoffmeister V., Kimeswenger S., Nielbock M., Nürnberger D., Schmidtbreick L., Sterzik M., 2004, *Nature*, 429, 155
 Chini R., Hoffmeister V. H., Kämpgen K., Kimeswenger S., Nielbock M., Siebenmorgen R., 2004, *A&A*, 427, 849
 Chini R., Wargau W. F., 1998, *A&A*, 329, 161
 Davis C. J., Nisini B., Takami M., Pyo T.-S., Smith M. D., Whelan E., Ray T. P., Chrysostomou A., 2006, *ApJ*, 639, 969
 Ducati J. R., Bevilacqua C. M., Rembold S. B., Ribeiro D., 2001, *ApJ*, 558, 309
 Fazio G. G. et al., 2004, *ApJS*, 154, 10
 Felli M., Massi M., Churchwell E., 1984, *A&A*, 136, 53
 Finger G., Biereichel P., Mehrgan H., Meyer M., Moorwood A. F., Nicolini G., Stegmeier J., 1998, in Fowler A. M., ed., *proc. SPIE 3354, Infrared detector development programs for the VLT instruments at the European Southern Observatory*. The International Society for Optical Engineering, p. 87
 Flaherty K. M., Pipher J. L., Megeath S. T., Winston E. M., Gutermuth R. A., Muzerolle J., Allen L. E., Fazio G. G., 2007, *ApJ*, 663, 1069
 Hartigan P., Heathcote S., Morse J. A., Reipurth B., Bally J., 2005, *AJ*, 130, 2197
 Hartung M. et al., 2003, in Iye M., Moorwood A. F. M., eds., *proc. SPIE 4841, CONICA design, performance and final laboratory tests*. The International Society for Optical Engineering, p. 425
 Heathcote S., Morse J. A., Hartigan P., Reipurth B., Schwartz R. D., Bally J., Stone J. M., 1996, *AJ*, 112, 1141
 Hoffmeister V. H., Chini R., Scheyda C. M., Nürnberger D., Vogt N., Nielbock M., 2006, *A&A*, 457, L29
 Hoffmeister V. H., Chini R., Scheyda C. M., Schulze D., Nürnberger D., Vogt N., 2008, *ApJ*, submitted
 Hollenbach D., McKee C. F., 1989, *ApJ*, 342, 306
 Ito M., Yamashita T., Sako S., Takami H., Hayano Y., Terada H., 2008, *ApJ*, 672, 398
 Itoh Y., 2001, in Zinnecker H., Mathieu R., eds., *proc. of IAU Symp. 200, Twisted Jets from L1551 IRS5*. The Astronomical Society of the Pacific, San Francisco, p. 261
 Jiang Z. et al., 2002, *ApJ*, 577, 245
 Krumholz M. R., Klein R. I., McKee C. F., 2007, *ApJ*, 656, 959
 Krumholz M. R., Thompson T. A., 2007, *ApJ*, 661, 1034
 Kumar M. S. N., Fernandes A. J. L., Hunter T. R., Davis C. J., Kurtz S., 2003, *A&A*, 412, 175
 Kurtz S., 2005, in Cesaroni R., Churchwell E., Felli M., Walmsley C. M., eds., *proc. IAU Symp. 227, Hypercompact HII regions*. Cambridge University Press, p. 111
 Nielbock M., Chini R., Müller S. A. H., 2003, *A&A*, 408, 245
 Nürnberger D. E. A., Chini R., Eisenhauer F., Kissler-Patig M., Modigliani A., Siebenmorgen R., Sterzik M. F., Szeifert T., 2007, *A&A*, 465, 931
 Pascucci I. et al., 2007, *ApJ*, 663, 383
 Reipurth B., Bally J., 2001, *ARAA*, 39, 403
 Román-Zúñiga C. G., Lada C. J., Muench A., Alves J. F., 2007, *ApJ*, 664, 357
 Rousset G. et al., 2003, in Wizinowich P. L., Bonaccini D., eds., *proc. SPIE 4839, NAOS, the first ao system of the VLT: on-sky performance*. The International Society for Optical Engineering, p. 140
 Russeil D., 2003, *A&A*, 397, 133
 Sako S. et al., 2005, *Nature*, 434, 995
 Siebenmorgen R., Krügel E., 2000, *A&A*, 364, 625
 Stark D. P., Whitney B. A., Stassun K., Wood K., 2006, *ApJ*, 649, 900
 Steinacker J., Chini R., Nielbock M., Nürnberger D., Hoffmeister V., Huré J.-M., Semenov D., 2006, *A&A*, 456, 1013
 Tielens A. G. G. M., Hollenbach D., 1985, *ApJ*, 291, 722
 Werner M. W. et al., 2004, *ApJS*, 154, 1
 Yorke H. W., Sonnhalter C., 2002, *ApJ*, 569, 846

This paper has been typeset from a \TeX / \LaTeX file prepared by the author.